



ORIGINAL RESEARCH

Open Access



# Multitemporal lidar captures heterogeneity in fuel loads and consumption on the Kaibab Plateau

Benjamin C. Bright<sup>1\*</sup> , Andrew T. Hudak<sup>1</sup>, T. Ryan McCarley<sup>2</sup>, Alexander Spannuth<sup>3</sup>, Nuria Sánchez-López<sup>2</sup>, Roger D. Ottmar<sup>4</sup> and Amber J. Soja<sup>5,6</sup>

## Abstract

**Background:** Characterization of physical fuel distributions across heterogeneous landscapes is needed to understand fire behavior, account for smoke emissions, and manage for ecosystem resilience. Remote sensing measurements at various scales inform fuel maps for improved fire and smoke models. Airborne lidar that directly senses variation in vegetation height and density has proven to be especially useful for landscape-scale fuel load and consumption mapping. Here we predicted field-observed fuel loads from airborne lidar and Landsat-derived fire history metrics with random forest (RF) modeling. RF models were then applied across multiple lidar acquisitions (years 2012, 2019, 2020) to create fuel maps across our study area on the Kaibab Plateau in northern Arizona, USA. We estimated consumption across the 2019 Castle and Ikes Fires by subtracting 2020 fuel load maps from 2019 fuel load maps and examined the relationship between mapped surface fuels and years since fire, as recorded in the Monitoring Trends in Burn Severity (MTBS) database.

**Results:** *R*-squared correlations between predicted and ground-observed fuels were 50, 39, 59, and 48% for available canopy fuel, 1- to 1000-h fuels, litter and duff, and total surface fuel (sum of 1- to 1000-h, litter and duff fuels), respectively. Lidar metrics describing overstory distribution and density, understory density, Landsat fire history metrics, and elevation were important predictors. Mapped surface fuel loads were positively and nonlinearly related to time since fire, with asymptotes to stable fuel loads at 10–15 years post fire. Surface fuel consumption averaged 16.1 and 14.0 Mg ha<sup>-1</sup> for the Castle and Ikes Fires, respectively, and was positively correlated with the differenced Normalized Burn Ratio (dNBR). We estimated surface fuel consumption to be 125.3 ± 54.6 Gg for the Castle Fire and 27.6 ± 12.0 Gg for the portion of the Ikes Fire (42%) where pre- and post-fire airborne lidar were available.

**Conclusions:** We demonstrated and reinforced that canopy and surface fuels can be predicted and mapped with moderate accuracy using airborne lidar data. Landsat-derived fire history helped account for spatial and temporal variation in surface fuel loads and allowed us to describe temporal trends in surface fuel loads. Our fuel load and consumption maps and methods have utility for land managers and researchers who need landscape-wide estimates of fuel loads and emissions. Fuel load maps based on active remote sensing can be used to inform fuel management decisions and assess fuel structure goals, thereby promoting ecosystem resilience. Multitemporal lidar-based consumption estimates can inform emissions estimates and provide independent validation of conventional fire emission

\*Correspondence: benjamin.c.bright@usda.gov

<sup>1</sup> Rocky Mountain Research Station, USDA Forest Service, 1221 S Main Street, Moscow, ID 83843, USA

Full list of author information is available at the end of the article

inventories. Our methods also provide a remote sensing framework that could be applied in other areas where airborne lidar is available for quantifying relationships between fuels and time since fire across landscapes.

**Keywords:** Forest fuels, Canopy fuels, Surface fuels, Fuel mapping, Fuel consumption, Post-fire fuel dynamics, Remote sensing, Airborne lidar

## Resumen

**Antecedentes:** La caracterización de la distribución física de los combustibles a través de paisajes heterogéneos es necesaria para entender el comportamiento del fuego, contabilizar las emisiones de humo, y manejar los ecosistemas para su resiliencia. Las mediciones mediante sensores remotos a varias escalas, aportan mapas para mejorar modelos de fuegos y dispersión de humos. Las mediciones con LIDAR aerotransportados que determinan directamente variaciones en altura y densidad de la vegetación, han probado ser especialmente útiles para el mapeo de la carga y el consumo de combustible a escala de paisaje. Predijimos la carga de combustibles en la planicie de Kaibab en el norte de Arizona, en los EEUU, estimamos el consumo a través de los incendios de Castle e Ikes de 2019, mediante la substracción de la carga de mapas de carga del 2020 menos los de 2019, y examinamos las relaciones entre el mapeo de los combustibles superficiales y años desde el fuego, registrados en la base de datos titulada Monitoreo de las Tendencias de la Severidad de los incendios (MTBS).

**Resultados:** Las correlaciones de  $R^2$  entre valores de cargas predichos y aquellos de observaciones de campo fueron 50, 39, 59, y 48% para combustible disponible en el dosel, combustibles de 1 a 1000h, mantillo y hojarasca por debajo del mantillo (duff), y combustible total superficial (la suma de combustibles de 1 a 1000h y del mantillo y la hojarasca subyacente), respectivamente. Las medidas del LIDAR que describían la distribución del dosel y su densidad, la densidad del sotobosque, las medidas históricas de fuego provistas por el Landsat y la altura (elevación) fueron predictores importantes. Las cargas de combustibles mapeadas fueron positivamente y no linealmente relacionadas al tiempo desde el fuego, con asíntotas hacia cargas de combustible estables entre 10 y 15 años post fuego. El consumo de la carga de combustibles en superficie promedió 16,1 y 14,0 Mg por ha para los incendios de Castle e Ikes, respectivamente y fue positivamente correlacionada con la diferencia normalizada de la relación de quema (dNBR). Estimamos que el consumo del combustible superficial fue de  $125,3 \pm 54,6$  Gg para el incendio de Castle y  $27,6 \pm 12,0$  Gg para la porción del incendio de Ikes (42%), del cual los datos de LIDAR aerotransportados (pre y post fuego), estaban disponibles.

**Conclusiones:** Demostramos y reforzamos que tanto el dosel como los combustibles superficiales pueden ser predichos y mapeados con una moderada precisión usando datos de LIDAR aerotransportados. Las medidas históricas de fuego provistas por el Landsat ayudaron a determinar la variación espacial y temporal de la carga de los combustibles superficiales y nos permitieron describir tendencias temporales en las cargas de combustible superficiales. Nuestros mapas y métodos de consumo y cargas de combustible son de utilidad para los gestores de recursos e investigadores que necesitan de estimaciones amplias de carga de combustible y emisiones a escala de paisaje. Los mapas de carga de combustibles basados en sensores remotos activos pueden ser usados para informar sobre decisiones de manejo de combustible y determinar metas de estructuras de cargas, promoviendo de esa manera la resiliencia del ecosistema. Las estimaciones de consumo basadas en LIDAR multitemporal pueden informar sobre estimaciones de emisiones y proveer de una validación de inventarios convencionales de emisiones por fuegos. Nuestros métodos también proveen de un marco conceptual de sensores remotos que pueden ser aplicados en otras áreas donde el LIDAR aerotransportado está disponible para cuantificar relaciones entre combustibles y tiempo desde el fuego en diferentes paisajes.

## Background

Land managers and researchers require fuel load measurements to manage fuels for ecosystem resilience (Covington et al. 1994; Graham et al. 2004), predict fire behavior (Countryman 1972; Alexander and Cruz 2013; Keane 2015), and quantify fire emissions (Seiler and

Crutzen 1980; Leenhouts 1998; French et al. 2004). Remote sensing data can facilitate spatially explicit estimates of fuel loads that would be difficult to obtain from inherently high heterogeneity fuel distributions that are impractical to characterize from in situ measurements alone (Keane et al. 2001; Arroyo et al. 2008; Keane 2015).

Integrated modeling methodologies often involve relating in situ measurements of fuel loads, such as tallies along transects (Brown 1974) or destructive samples (Hawley et al. 2018), to remotely sensed data and other ancillary data sources that provide synoptic coverage (Keane et al. 2001). For many applications, such as landscape-level management of fuels, fuel load estimates at coarser spatial scales (20 to 30 m) are sufficient and perhaps preferred (e.g., Rollins 2009; Reeves et al. 2009). For some recent fire science investigations using physically based models, more highly resolved, three-dimensional representations of fuel loads are needed to better model and understand fire behavior (Hiers et al. 2009, 2020; Rowell et al. 2016). Because fuels are dynamic in space and time, especially following disturbance, methods that quantify the relationship between fuel loads and time since disturbance are needed to monitor and model fuel accumulation across landscapes. Methods modeling the dynamic relationships between disturbance and fuel loading over space and time can alleviate the need for annual fuel loading monitoring efforts. Such methods can also help wildland fire managers assess potential fire behavior with geospatial fire history information which is common in many national forests around the United States. Mapping and assessing the heterogeneous fuel loading trajectories across a given landscape can help planning efforts aimed at preventing undesirable impacts to human and natural communities.

Light detection and ranging (lidar) actively measures live and dead vegetation structure and is therefore particularly well-suited, relative to passive optical sensors, for quantifying forest fuel loads at various spatial scales and height strata (Arroyo et al. 2008); common fuel strata definitions include canopy, shrub, herbaceous, downed woody, litter, and duff layers (Ottmar et al. 2007). Terrestrial lidar, in which the lidar sensor is mounted on or near ground level, has been used to estimate canopy, shrub, and herbaceous fuel loads at fine spatial scales (spatial resolutions of 1 m or less, e.g., Loudermilk et al. 2009; Skowronski et al. 2011; Hudak et al. 2020, Rowell et al. 2020). To generate coarser-scale fuel load maps (spatial resolutions of 20 m or greater) of various fuel strata across landscapes, airborne lidar is commonly used (e.g., Andersen et al. 2005; Erdody and Moskal 2010; Hermosilla et al. 2013; Hudak et al. 2015, 2016). Spaceborne lidar has also been applied to mapping of various fuel strata (e.g., García et al. 2012; Peterson et al. 2013; Leite et al. 2022). When pre- and post-fire lidar data are available, fuel load estimates can be differenced to estimate consumption (McCarley et al. 2020; Hudak et al. 2020), which can be useful for investigating fire effects and fuel-fire-emissions relationships (Hudak et al. 2015; McCarley et al. 2020).

Previous studies using airborne and spaceborne lidar for fuel load estimation have most often predicted canopy fuel loads. Subcanopy (shrub, herbaceous, downed woody, litter, and duff) fuel loads have been predicted less often and less accurately (Seielstad and Queen 2003; Pesonen et al. 2008; Jakubowski et al. 2013; Hudak et al. 2015, 2016; Price and Gordon 2016; Bright et al. 2017; Stefanidou et al. 2020; McCarley et al. 2020; Mauro et al. 2021; Alonso-Rego et al. 2021; Leite et al. 2022). Limitations to measuring subcanopy fuels include (1) occlusion and attenuation by the overstory so that near-ground fuel structure is sampled unreliably, (2) insufficient horizontal point density and/or vertical accuracy (often ~15 cm) to quantify near-surface fuel heights, (3) inability to directly measure litter and duff depth, and (4) the often intrinsic, high heterogeneity of subcanopy fuels across space that makes reliable in situ sampling and therefore modeling difficult (Keane et al. 2001; Keane 2015). Despite these challenges, previous studies have reported useful prediction accuracies and have concluded that subcanopy fuel load estimates derived from airborne and spaceborne lidar have utility for managers.

Here we predicted and mapped available canopy fuel (foliage weight plus 50% of small branch weight) and surface fuels (downed woody, litter, and duff) across a landscape in northern Arizona, USA, using in situ field observations, multitemporal airborne lidar, and Landsat-derived fire history metrics (number of past fires (NPF) and years since fire (YSF)). By differencing pre- and post-fire fuel load maps, we estimated fuel consumption for two fires, the Castle and Ikes Fires of 2019. Few previous studies have estimated fuel consumption across a landscape with multitemporal airborne lidar (e.g., Wang and Glenn 2009; Alonzo et al. 2017; Hoe et al. 2018; Hu et al. 2019; Skowronski et al. 2020; McCarley et al. 2020). We also examine the relationship between lidar-derived surface fuel load maps and fire history and present a remote sensing framework for quantifying temporal dynamics in surface fuel accumulation, which, to our knowledge, no previous study has done.

## Methods

### Study area

Our study area spanned the Kaibab Plateau on the north rim of the Grand Canyon in northern Arizona, USA (Fig. 1), which is administered by the United States National Park Service (USNPS) and United States Forest Service (USFS). Annual precipitation increases with elevation to dictate dominant vegetation type across the plateau, with shrublands occurring at lower elevations (minimum of 860 m in our study area), woodlands occurring at intermediate elevations, and forests occurring at higher elevations (maximum of 2800 m in our study area).

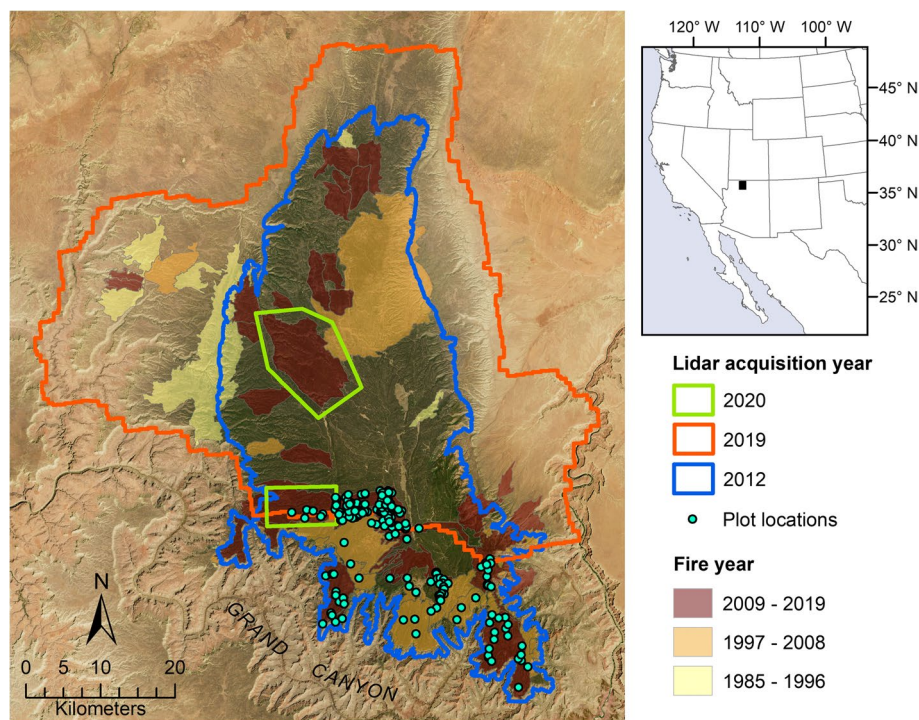


**Fig. 1** The Kaibab Plateau in northern Arizona overlaid with airborne lidar extents and past fire perimeters from the Monitoring Trends in Burn Severity (MTBS) database. The 2020 lidar was two parcels acquired across the entire 2019 Castle Fire (within the northern 2020 lidar polygon) and a portion of the 2019 Ikes Fire (within the southern 2020 lidar rectangle). True-color background imagery is from Landsat 8

Forest types across the plateau, in order of ascending elevation, include piñon-juniper woodlands (*Pinus edulis* Engelm., *Pinus monophylla* Torr. & Frem., *Juniperus osteosperma* (Torr.) Little, approx. 1370–2290 m), ponderosa pine woodlands and forests (*Pinus ponderosa* Lawson & C. Lawson, approx. 1950–2600 m), and mixed conifer forest (*Pinus ponderosa*, *Pseudotsuga menziesii* [Mirb.] Franco, *Picea engelmannii* Parry ex Engelm., *Abies lasiocarpa* [Hook.] Nutt., *Abies concolor* (Gord. & Glend.) Lindl. ex Hildebr., *Picea pungens* Engelm., *Populus tremuloides* Michx., approx. 2380–3000 m), with spruce-fir forests (*Picea engelmannii*, *Abies lasiocarpa*, approx. >2500 m) dominating the highest elevations (United States Department of the Interior (USDOI) National Park Service 2010). At lower elevations at the base of the plateau, annual precipitation averages 370 mm, summer maximum temperatures average 19.4°C, and winter minimum temperatures average 4.5°C; at higher elevations on the plateau, annual precipitation averages 710 mm, summer maximum temperatures average 14.3°C, and winter minimum temperatures average –0.3°C (30-year normals for 1981–2010; <https://prism.oregonstate.edu/normals/>). Wildfire frequents the plateau (Fig. 1). In general, fires have historically been more frequent and lower in severity in ponderosa

pine forest, and less frequent and of mixed severity in higher elevation forest types (Fulé et al. 2003a, b). Both planned and unplanned fire events are being used to restore ecosystem resilience and function to these fire-adapted ecosystems. Kaibab National Forest managers are actively restoring historic fire return intervals in ponderosa pine (Fire Regime I, 0–35 years) and mixed conifer (Fire Regimes III, IV, V, 35–200 years) forests of the Kaibab Plateau (USDA Forest Service 2014, 2020).

#### Field observations

The USNPS and USFS maintain a field plot network to monitor and assess fire effects on vegetation and fuels within Grand Canyon National Park and the adjoining Kaibab National Forest (USDOI National Park Service 2010); field plot data are shared between the two federal agencies. Overstory trees are monitored on fixed-radius plots (area = 0.03 ha, radii = 10 m). For each tree with a diameter at breast height (DBH) > 15 cm, the following is periodically recorded: status (live or dead), DBH, species, height, live crown base height, and crown class (dominant, codominant, intermediate, subcanopy). Surface (downed woody, litter, and duff) fuels are monitored using one or two 15.24-m (50-ft) transects, with one end of the transect located at the center of the

fixed-radius overstory plots. Both 1-h and 10-h fuels are measured along the first 1.83 m (6 ft) of transects, 100-h fuels are measured along the first 3.66 m (12 ft) of transects, and 1000-h fuels are measured along the entire length of the transects. Litter and duff depth are recorded at every 1.52 m (5 ft) along the length of transects. Transect starting point locations are recorded with professional-grade GNSS receivers and differentially corrected, resulting in expected horizontal accuracies of <1 m. Overstory fixed-radius plot centers can be derived from these transect starting point locations.

We used a subset of overstory tree ( $N=69$ ) and surface fuel ( $N=153$ ) plot data that were spatially and temporally coincident (field observations taken within 2 years of airborne lidar acquisition) with 2012 and 2019 airborne lidar data for model development. Plots disturbed by fire between time of field measurement and lidar acquisition were not included. Available canopy fuel, defined as foliage weight plus 50% of small branch weight, was calculated allometrically for the overstory plots by implementing Appendix D of the FuelCalc User Guide in R (Reinhardt et al. 2006; Lutes 2021). Surface fuel transect tallies and depth measurements were converted to surface fuel density measurements following Brown et al. (1982) and averaged by plot.

#### Airborne lidar data

Airborne lidar were acquired across 1853 and 2944 km<sup>2</sup> of the Kaibab Plateau in 2012 and 2019, respectively (Fig. 1; Table 1). The 2012 lidar extent covered forested lands within the North Kaibab District of the Kaibab National Forest, as well as a portion of Grand Canyon National Park. The 2019 lidar extent spanned the entire North Kaibab District of the Kaibab National Forest. To

measure fire-caused change and post-fire vegetation conditions, two smaller acquisitions totaling 175 km<sup>2</sup> were made in 2020 across the entire 2019 Castle Fire extent and a portion of the 2019 Ikes Fire extent (42% coverage by 2019 and 2020 lidar). The Castle and Ikes Fires were 78 km<sup>2</sup> and 67 km<sup>2</sup> in size, respectively. Point cloud data, with points classified as ground or nonground, were delivered by vendors as tiled LAS files.

Point cloud data were processed to create vegetation metrics with the LAStools (Isenburg 2021) and R (R Core Team 2021) software packages. Points were normalized to heights above ground with the “lasheight” LAStools function and vegetation metrics were calculated with “lascanopy” LAStools function (Table 2). Metrics were calculated for circular fixed-radius (radii = 10 m) overstory plot extents coincident with 2012 and 2019 lidar data ( $N=69$ ), and for circular areas encompassing 15.24-m surface fuel transects ( $N=153$ ), to be used for predictive modeling. Metric grids with a spatial resolution of 20 m were also created by binning lidar points into 20-m grid cells (step = 20) across lidar extents with “lascanopy.” These grids were used for mapping. Topographic metrics based on vendor-supplied digital terrain models (DTM) were created at 20-m spatial resolution with the “raster” and “spatialEco” R packages (Table 2; Hijmans 2021a; Evans 2021). Topographic metric values at plot locations were extracted for use in predictive modeling.

#### Landsat fire history data

We used the Monitoring Trends in Burn Severity (MTBS) database (1984–2019; Eidenshink et al. 2007) coincident with the study area (Fig. 1) to create years-since-fire (YSF) and number-of-past-fire (NPF) grids for the years 2012 and 2019. Grids were created by converting MTBS

**Table 1** Airborne lidar acquisition parameters for each acquisition

Parameter	Acquisition year		
	2012	2019	2020
Vendor	Watershed Sciences, Inc.	Atlantic	Technical Applications & Consulting, LLC
Platform	Cessna Caravan	PACVX (N750VX)	Cessna Turbo Utility 206
Sensor	Leica ALS50 Phase II and ALS60	Optech Galaxy Prime	Optech Galaxy T500
Acquisition dates	Aug. 25–Sept. 15, 2012	June 27–Jul. 3, 2019	Sept. 30–Oct. 2, 2020
Survey Altitude (AGL)	900–2000 m	1800 m	961–1066 m
Footprint diameter	21–45 cm	45 cm	24–27 cm
Scan frequency	49–66 Hz	53 Hz	110–113 Hz
Pulse rate of scanner	50–106 kHz	450 kHz	550 kHz
Laser wavelength	1064 nm	1064 nm	1064 nm
Mean pulse density	≥ 8 pulses m <sup>-2</sup>	≥ 8 pulses m <sup>-2</sup>	9–20 pulses m <sup>-2</sup>
Total area surveyed	1853 km <sup>2</sup>	2944 km <sup>2</sup>	175 km <sup>2</sup>

**Table 2** Vegetation and topography metrics, derived from airborne lidar, and fire history metrics, derived from the Monitoring Trends in Burn Severity (MTBS) database. Metrics were candidate predictor variables for random forest (RF) models predicting fuel loads. Nonground returns are defined as those > 0 m above ground. Canopy returns are defined as those > 2 m above ground. Understory returns are defined as those > 0 and < 2 m above ground

Metric name	Description
MAX.gt2	Maximum height of canopy returns
AVG.gt2	Mean height of canopy returns
STD.gt2	Standard deviation of canopy return heights
SKE.gt2	Skewness of canopy return heights
KUR.gt2	Kurtosis of canopy return heights
P05.gt2	5th percentile of canopy return heights
P10.gt2	10th percentile of canopy return heights
P25.gt2	25th percentile of canopy return heights
P50.gt2	50th percentile of canopy return heights
P75.gt2	75th percentile of canopy return heights
P90.gt2	90th percentile of canopy return heights
P95.gt2	95th percentile of canopy return heights
MAX.lt2	Maximum height of understory returns
AVG.lt2	Mean height of understory returns
STD.lt2	Standard deviation of understory return heights
SKE.lt2	Skewness of understory return heights
KUR.lt2	Kurtosis of understory return heights
P05.lt2	5th percentile of understory return heights
P10.lt2	10th percentile of understory return heights
P25.lt2	25th percentile of understory return heights
P50.lt2	50th percentile of understory return heights
P75.lt2	75th percentile of understory return heights
P90.lt2	90th percentile of understory return heights
P95.lt2	95th percentile of understory return heights
D00	Percentage of nonground returns 0–0.5 m above ground
D01	Percentage of nonground returns 0.5–1 m above ground
D02	Percentage of nonground returns 1–2 m above ground

**Table 2** (continued)

Metric name	Description
D03	Percentage of nonground returns 2–4 m above ground
D04	Percentage of nonground returns 4–8 m above ground
D05	Percentage of nonground returns 8–16 m above ground
D06	Percentage of nonground returns 16–32 m above ground
D07	Percentage of nonground returns 32–48 m above ground
D00.lt2	Percentage of understory returns 0–0.05 m above ground
D01.lt2	Percentage of understory returns 0.05–0.15 m above ground
D02.lt2	Percentage of understory returns 0.15–0.5 m above ground
D03.lt2	Percentage of understory returns 0.5–1 m above ground
D04.lt2	Percentage of understory returns 1–2 m above ground
CURV.plan	Planform curvature (Zevenbergen and Thorne 1987)
CURV.profile	Profile curvature (Zevenbergen and Thorne 1987)
CURV.total	Total curvature (Zevenbergen and Thorne 1987)
DEM	Elevation
HLI	Heatload index (Eq. 3 of McCune and Keon 2002)
SLOPE	Slope (degrees)
SCOSA	Slope * cosine(aspect) (Stage 1976)
SSINA	Slope * sin(aspect) (Stage 1976)
TPI	Topographic position index (Hijmans 2021a)
TRASP	Transformed aspect $(1 - \cos(\text{aspect} - 30)) / 2$ (Roberts and Cooper 1989)
TRI	Topographic roughness index (Wilson et al. 2007)
YSF	Years since fire (derived from the MTBS database, 1984–2019)
NPF	Number of past fires (derived from the MTBS database, 1984–2019)

polygons representing fire perimeters to 20-m raster format and performing raster calculations with the “terra” package in R (Hijmans et al. 2021b). YSF and NPF values were extracted at plot locations to be used as additional predictor variables, and YSF and NPF grids were used for mapping.

#### Random forest modeling

We predicted canopy and surface fuels from airborne lidar and Landsat-derived fire history metrics using

random forest (RF) modeling implemented in the “randomForest” package of R (Breiman 2001; Liaw and Wiener, 2002; R Core Team 2021). Response variables included available canopy fuel, 1- to 1000-h fuels, litter and duff, and total surface fuel (sum of 1- to 1000-h, litter and duff fuels). Candidate predictor variables included the airborne lidar and fire history metrics listed in Table 2.

For each response variable, we identified the most important predictor variables using the “rf.modelSel” routine of the “rfUtilities” R package (Evans and Murphy 2018; Murphy et al. 2010), which computes normalized predictor variable importance scores (MIR) that range from 1 (most important) to zero (least important). To reduce possible bias towards selection of highly correlated predictor variables (Strobl et al. 2008), we considered only one predictor variable of highly correlated predictor variable pairs or sets ( $r > 0.9$ ) when running the “rf.modelSel” routine, which we ran with various predictor variable sets. RF models were run in regression mode with the default values of 500 trees ( $n_{tree} = 500$ ) and the number of variables at each node split set to the total number of candidate predictor variables ( $p$ ) divided by three ( $m_{try} = p/3$ ). Model performance was assessed with out-of-bag error estimates. Final RF models for each of the four response variables included only the most important, not highly correlated, predictor variables.

### Fuel map creation and analysis

Final RF models predicting available canopy fuel and total surface fuel were applied to 20-m metric grids to create maps of these two fuel variables across each lidar acquisition (years 2012, 2019, 2020). We analyzed 2012 and 2019 predicted fuel maps by time since fire, as recorded by MTBS-derived YSF grids, and forest type, as mapped by LANDFIRE Existing Vegetation Type (EVT) grids (LANDFIRE 2014, 2016). We explored linear and various nonlinear models for describing relationships between predicted fuel maps and YSF.

Consumption was estimated across the 2019 Castle Fire extent and a portion of the 2019 Ikes Fire extent by differencing 2019 and 2020 predicted fuel maps. To test whether consumption was related to burn severity, we compared consumption grids with MTBS differenced Normalized Burn Ratio (dNBR) grids, indicators of burn severity (Key and Benson 2006). Total and average consumption for the Castle Fire and portion of the Ikes Fire were estimated by summing and averaging mapped consumption estimates within fire extents. Confidence intervals for total consumption were created by multiplying total consumption estimates by percent root mean square error (%RMSE) values from RF models. %RMSE was defined as the square root of the mean of the squared

residuals, divided by the mean of the observed fuel values. Grid cells within the 2018 Stina Fire extent were excluded from the calculation of consumption averages and totals for the Ikes Fire.

## Results

### Random forest models predicting fuel loads

Available canopy fuel ranged from 0.9 to 16.5  $Mg\ ha^{-1}$  and averaged 6.9  $Mg\ ha^{-1}$  across the 69 fixed-radius plots. Our RF model explained 50% of the variation in available canopy fuel (Fig. 2). Variables describing canopy height distribution (SKE.gt2, KUR.gt2, P10.gt2, P50.gt2) and density of lower vegetation (D00, D03, D02.lt2) as well as one topographic interaction variable between slope and aspect (SSINA) were important predictors of available canopy fuel (Table 3).

Across the 153 fuel transects, 1- to 1000-h fuels ranged from 2.1 to 178.6  $Mg\ ha^{-1}$  and averaged 45.8  $Mg\ ha^{-1}$ , duff and litter ranged from 1.4 to 103.6  $Mg\ ha^{-1}$  and averaged 36.9  $Mg\ ha^{-1}$ , and total surface fuels ranged from 7.7 to 237.6  $Mg\ ha^{-2}$  and averaged 82.7  $Mg\ ha^{-1}$ . RF models explained 39% of the variation in 1- to 1000-h fuels, 59% of the variation in litter and duff, and 48% of the variation in total surface fuels (Fig. 2). Lower canopy height (P05.gt2), understory density (D01, D00.lt2), elevation (DEM), and number of past fires (NPF) were important predictors of 1- to 1000-h fuels that were included in the final RF model (Table 3). Understory (D00) and canopy (D03, D06) density, elevation (DEM), and fire history (YSF, NPF) variables were important predictors of litter and duff (Table 3). Important predictors of total surface fuels included in the final model were lower canopy height (P10.gt2), understory height (P90.lt2), understory density (D02.lt2, D03.lt2), elevation (DEM), and fire history (YSF, NPF) variables (Table 3).

### Fuel and consumption map analyses

Predicted available canopy fuel maps varied with LANDFIRE EVT as expected, with greater available canopy fuels in ponderosa pine, mixed-conifer, and spruce-fir forests on the Kaibab Plateau, and less available canopy fuels in piñon-juniper woodlands and shrublands at lower elevations (Fig. 3). There was no significant relationship between available canopy fuel and years since fire.

Predicted total surface fuel maps showed variation related to LANDFIRE EVT and fire history; ponderosa pine forests and recently burned areas tended to have lower total surface fuel loads (Fig. 3). Total surface fuel loads were positively and significantly related to years since fire (Fig. 4). Three-parameter asymptotic models described the relationship between predicted total surface fuels and years since fire slightly better than linear

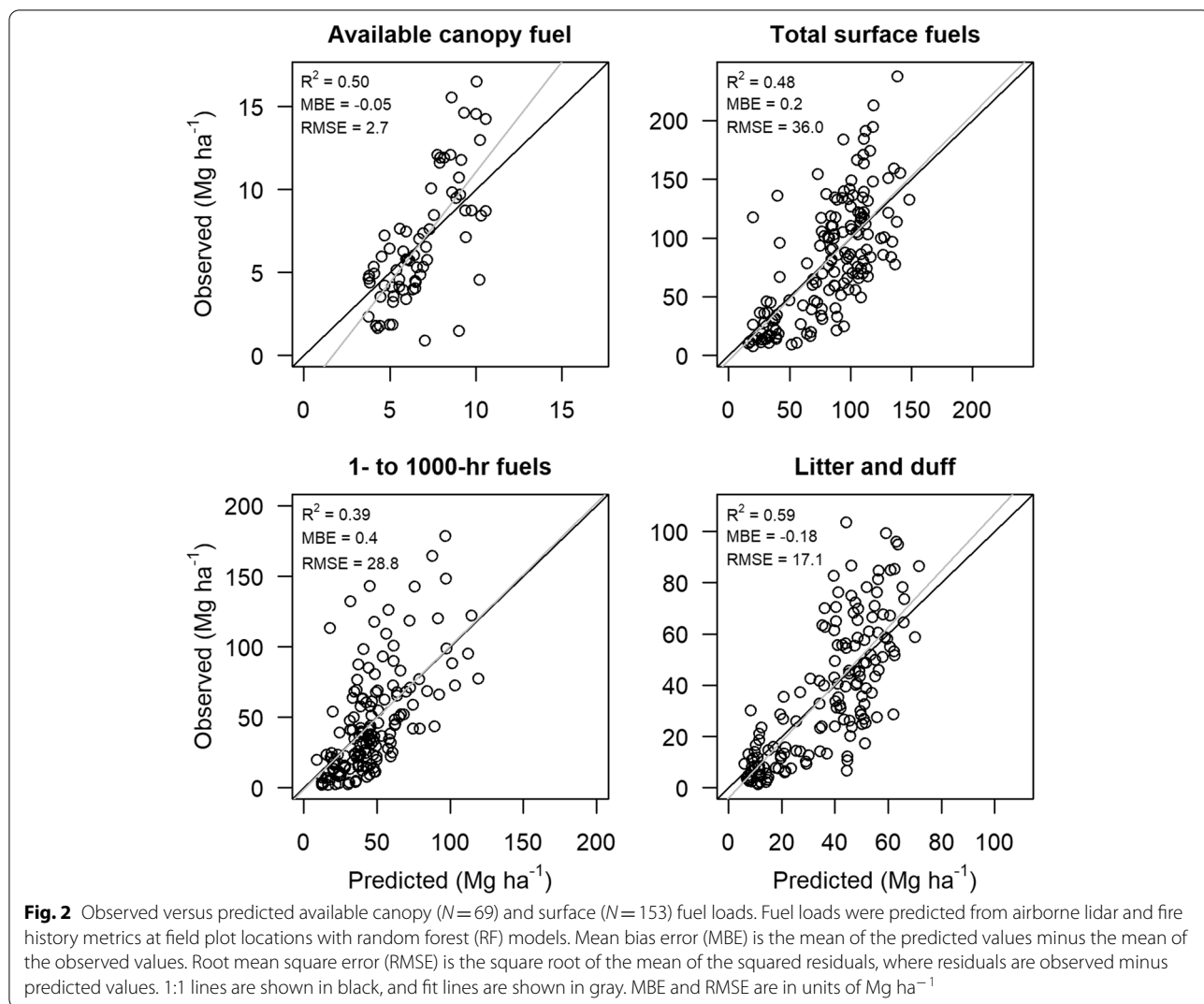


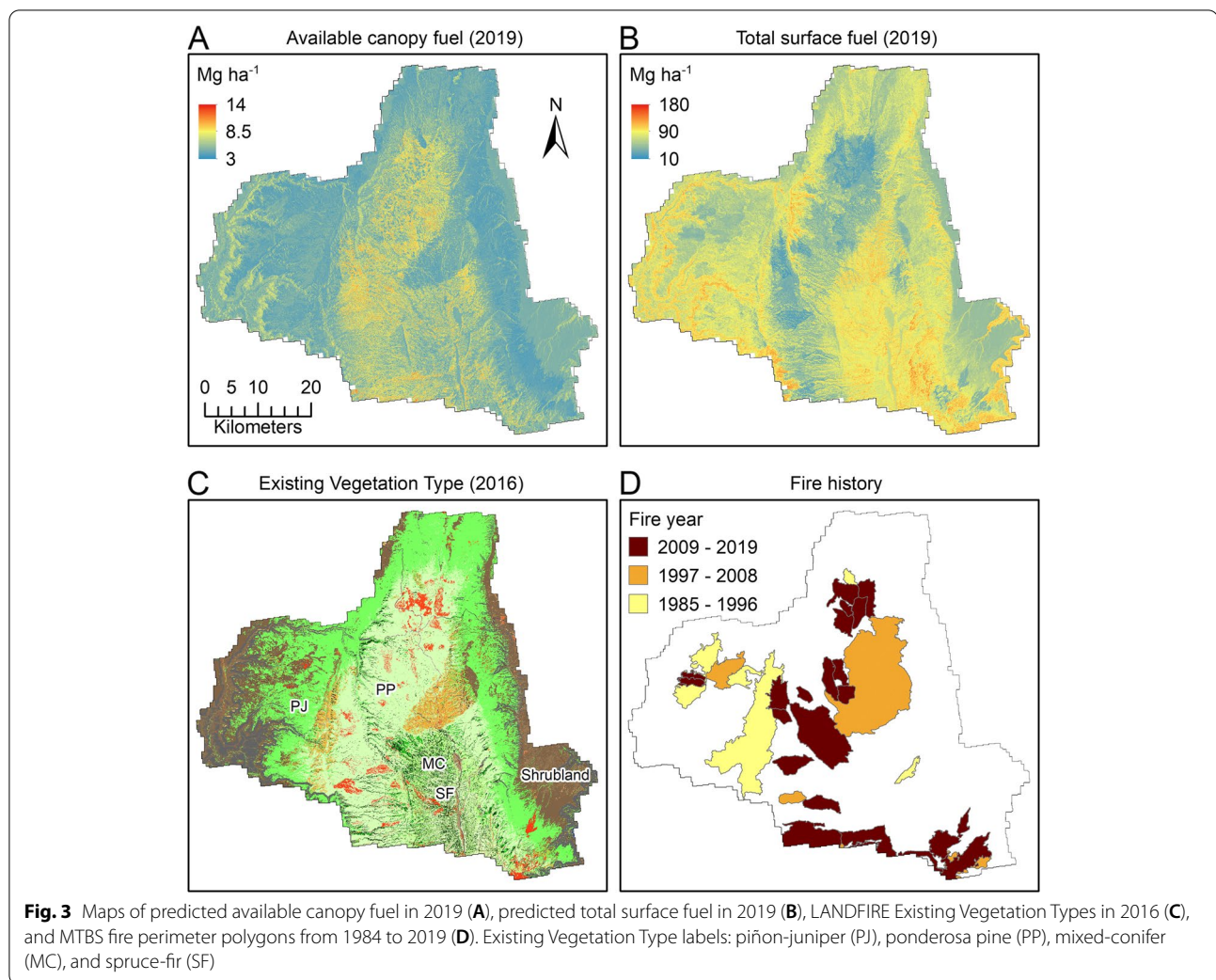
**Table 3** Important predictors included in final models and percent variance explained for each fuel response variable. Predictor variables are ordered by importance, and normalized predictor variable importance scores (MIR) ranging from 1 (most important) to zero (least important) are given in parentheses after each predictor variable. See Table 2 for predictor variable definitions

Response variable	Important predictors	Var. Exp. (%)
Available canopy fuel	P10.gt2 (1), SKE.gt2 (0.6), D03 (0.6), P50.gt2 (0.5), KUR.gt2 (0.4), D00 (0.4), D02.lt2 (0.3), SSINA (0.3)	50
1- to 1000-h fuels	DEM (1), P05.gt2 (1), D01 (0.6), D00.lt2 (0.6), NPF (0.3)	39
Litter and duff	DEM (1), YSF (0.6), NPF (0.4), D06 (0.3), D03 (0.3), D00 (0.2),	59
Total surface fuel	DEM (1), D03.lt2 (0.6), D02.lt2 (0.5), P90.lt2 (0.5), P10.gt2 (0.5), YSF (0.3), NPF (0.2)	48

models, with  $R^2$  values ranging from 0.10 to 0.23. The response of surface fuel to time since fire followed an asymptote towards stable fuel levels of approximately  $90\text{--}130\text{Mg}\text{ha}^{-1}$  at 10–15 years post-fire (Fig. 4). More observations (20-m pixels) were available in areas that burned between 1 and 15 years previously, with

relatively fewer observations available for areas that burned > 15 years previously.

Predicted surface fuel consumption averaged  $16.1$  and  $14.0\text{Mg}\text{ha}^{-1}$  for the Castle and Ikes Fires, respectively (Fig. 5). Total surface fuel consumed by the Castle Fire and the portion of the Ikes Fire where



pre- and post-fire lidar data were available was estimated to be  $125.3 \pm 54.6$  and  $27.6 \pm 12.0$  Gg, respectively. Predicted canopy fuel consumption averaged  $-0.3 \text{ Mg ha}^{-1}$  across both fires, i.e., on average, available canopy fuel increased between 2019 and 2020. For areas that burned at high severity, predicted canopy fuel consumption averaged 0 and  $0.09 \text{ Mg ha}^{-1}$  for the Castle Fire and portion of the Ikes Fire, respectively. Predicted canopy fuel consumption for the portion of the Ikes Fire totaled  $0.003 \pm 0.001$  Gg. The 2018 Stina Fire extent (not included in consumption averages and totals) was apparent in the 2019 Ikes Fire extent as an area of “negative” consumption (Fig. 5).

Surface fuel consumption grids were positively correlated with the dNBR grids, with Pearson correlation coefficients of 0.33 and 0.37 for the Castle and Ikes Fires, respectively (Fig. 5). Average predicted surface fuel consumption varied by MTBS burn severity class, with smallest average consumption in the

unburned-to-low severity class and greatest average consumption in the high severity class (Table 4). Canopy fuel consumption and dNBR grids were uncorrelated, with Pearson correlation coefficients of 0 and 0.04 for the Castle and Ikes Fires, respectively.

## Discussion

Our results show an encouraging improvement in estimating and mapping fuel loads and consumption with airborne lidar, especially for subcanopy fuels that have been poorly characterized with remote sensing in the past. We predicted canopy and surface fuel loads with moderate accuracy (39–59%) including both airborne lidar and fire history predictor variables. Our analysis focused on surface fuel loads because fewer previous studies have predicted surface fuels with airborne lidar, and because canopy fuel available for burning was much smaller relative to surface fuel in our study area. Our moderate accuracies for surface fuel load prediction with

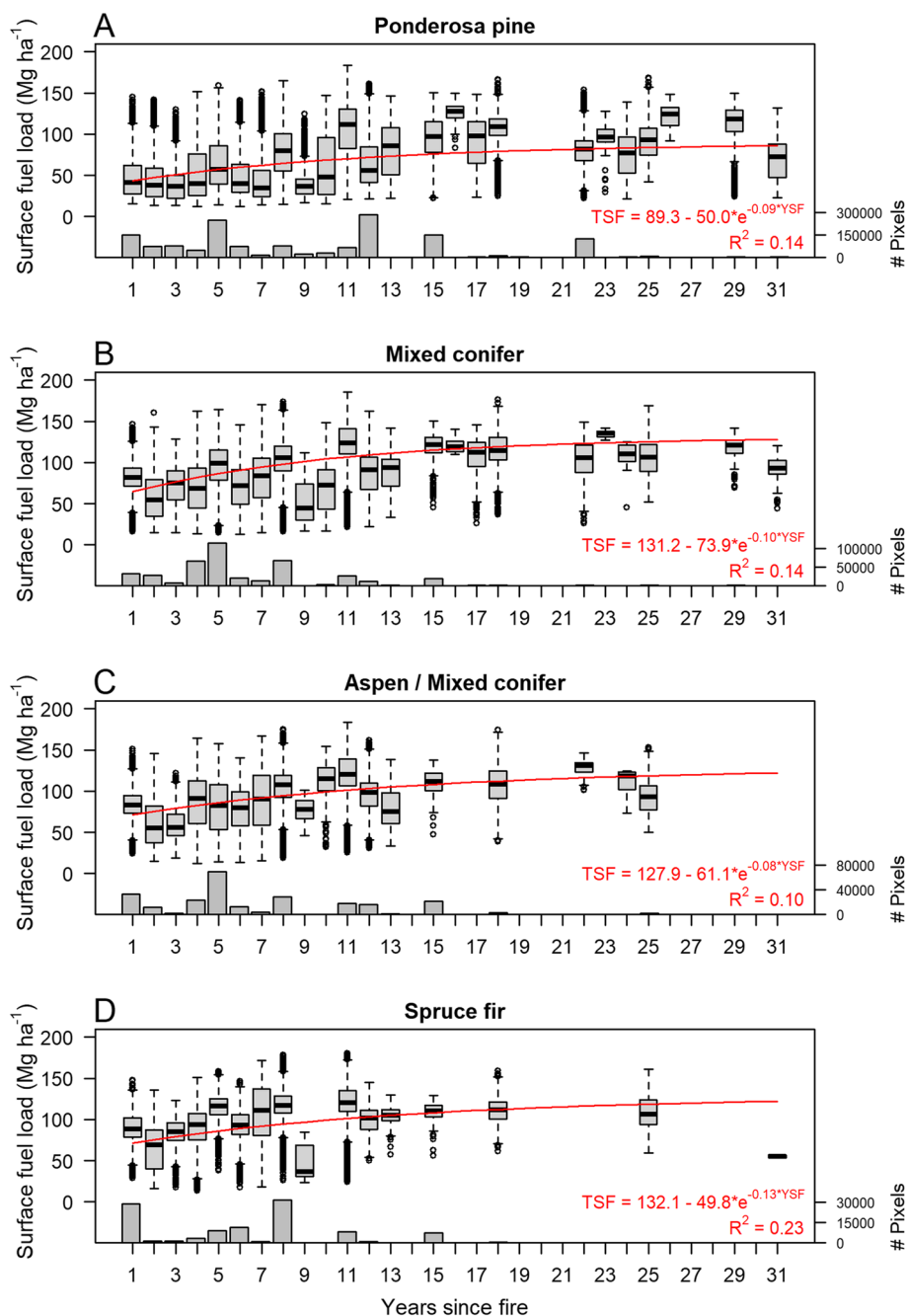
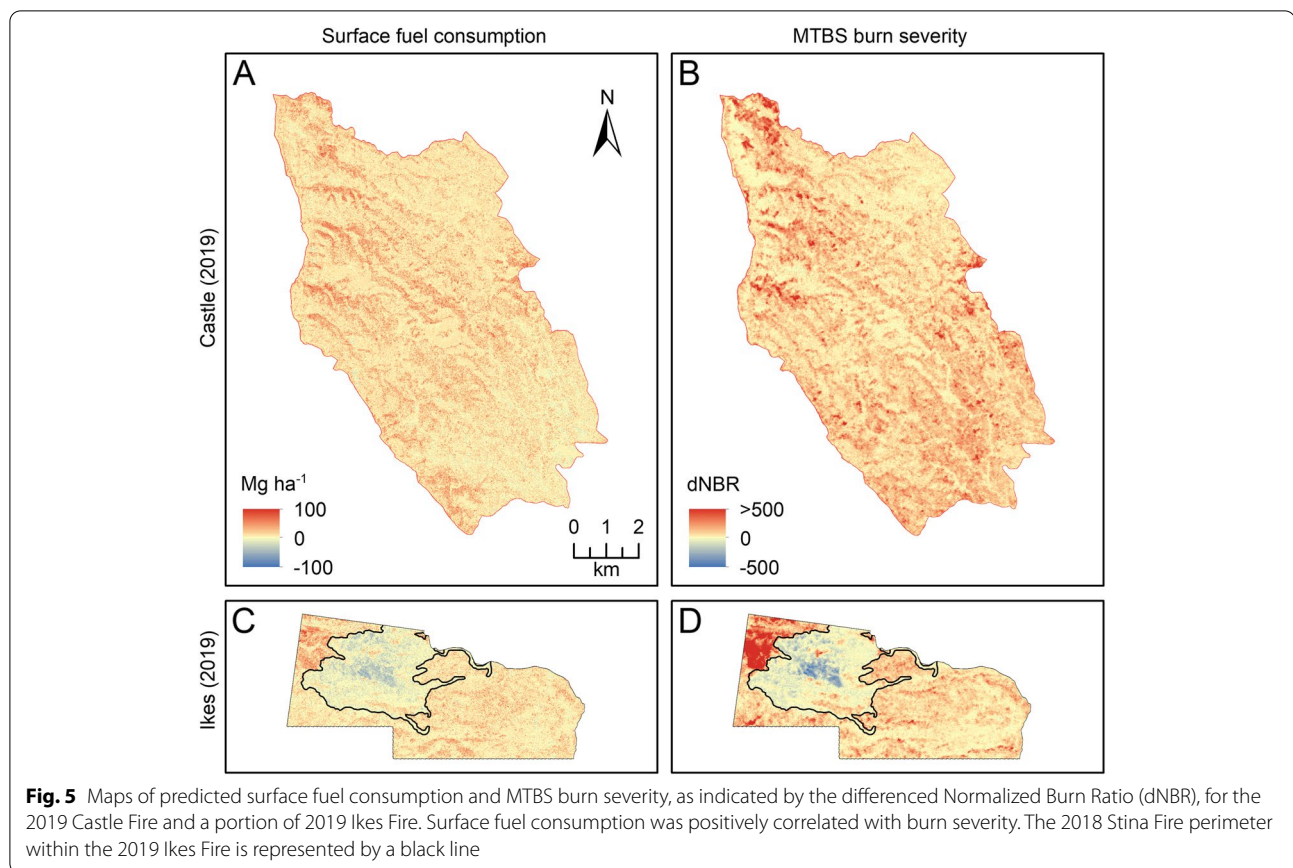


**Fig. 4** Time series of surface fuel loads derived from overlaying 2012 and 2019 predicted surface fuel load (TSF) maps with years since fire (YSF) grids created from the Monitoring Trends in Burn Severity (MTBS) database (1984–2019). Predicted surface fuel loads increased with years since fire, with asymptotes where fuel accumulation slowed at approximately 10–15 years post fire. Fit lines for three-parameter asymptotic models are shown as red lines. The number of 20-m pixels that went into each distribution is quantified in bars at the bottom of each panel

airborne lidar are comparable to those of past studies (Table 5).

Our RF models showed relatively high predictive power for low fuel loads but showed a trend of increased error and underprediction for higher fuel loads (Fig. 2).

Although nonparametric RF models do not require normally distributed variables, underprediction at the high end of fuel gradients might have been caused by field data being skewed toward the lower end of fuel gradients. Most field data were collected at 10 years or less post-fire,



for the intent of monitoring post-fire recovery. Including more field sampling at the higher end of fuel gradients in areas that had not recently burned might have helped to alleviate this increased error and under prediction of higher fuel loads. We were, however, limited to using field data that were not gathered for the intent of our modeling analysis, nor did we try to balance samples by excluding any of the limited number of available field observations.

RF models predicting surface fuel loads included both near surface (0–2 m aboveground) and overstory (> 2 m

above ground) predictor variables, indicating that airborne lidar both directly measured variation in near surface fuels and indirectly captured surface fuel variation through overstory correlates. Our RF model predicting litter and duff, which cannot be directly measured with airborne lidar as it does not penetrate the ground surface, especially demonstrates the potential of using overstory correlates to estimate underlying surface fuels. Others have also found that overstory correlates are helpful for predicting surface fuel variables with airborne lidar (Price and Gordon 2016; Bright et al. 2017; Stefanidou et al. 2020; McCarley et al. 2020) and have documented relationships between overstory characteristics and surface fuel loads (Prescott 2002; Lydersen et al. 2015; López-Senespleda et al. 2021).

One topographic variable, elevation, was an especially important predictor of surface fuel loads across our study area on the Kaibab Plateau in Arizona. Surface fuel increased with elevation, and we predicted smaller surface fuel loads in ponderosa pine forests relative to higher elevation forest types. This pattern is likely because of increasing annual precipitation with elevation that results in greater vegetation growth, ecosystem productivity, and therefore fuel loads. Environmental gradients such as elevation, when

**Table 4** Average and standard deviation (in parentheses) of predicted surface fuel consumption, in  $\text{Mg ha}^{-1}$ , by MTBS burn severity class for the 2019 Castle and Ikes Fires

MTBS burn severity class	Fire	
	Castle	Ikes
Unburned to low	10.7 (11.3)	8.7 (12.0)
Low	17.5 (15.8)	15.6 (15.6)
Moderate	29.6 (19.3)	29.8 (20.3)
High	41.5 (21.4)	30.1 (19.0)

**Table 5** Other studies predicting surface fuel variables from airborne lidar

Authors	Year	Forest type	Location	Surface fuel response variable(s)	Variance explained (%)
Pesonen et al.	2008	Spruce and hardwood	Finland	Downed dead wood volume	61
Jakubowski et al.	2013	Mixed conifer	California, USA	1000-h fuel load, fuel bed depth	31, 35
Hudak et al.	2015	Longleaf pine savanna	Florida, USA	In(surface fuel load)	44
Price and Gordon	2016	Dry Sclerophyll Forest	Australia	Surface fuel load	24
Bright et al.	2017	Pine and spruce-fir	Colorado, USA	Litter and duff, 1- to 100-h, 1000-h, and total surface fuel loads	24–32
Stefanidou et al.	2020	Fir	Greece	Transformed litter, grass/forbs, 1-h, 10-h, and total surface fuel loads	60–71
McCarley et al.	2020	Conifer	New Mexico and Oregon, USA	Understory fuel load	16–63
Mauro et al.	2020	Conifer	Oregon, USA	Downed woody biomass	14
Alonso-Rego et al.	2021	Pine	Spain	Understory fuel, litter and duff, and downed woody debris loads	35–42
Bright et al. (this study)	2022	Pine, mixed-conifer, spruce-fir	Arizona, USA	Litter and duff, 1- to 1000-h and total surface fuel loads	39–59

combined with other data sources, have proven to be useful in other fuel mapping efforts (Keane et al. 2000, 2001; Reich et al. 2004; Pierce et al. 2012; Lin et al. 2021).

Predicted surface fuel loads varied significantly with time since fire, as measured by MTBS Landsat products, across our study area (Fig. 4). Although Landsat-derived fire history variables were not as important as lidar variables describing vegetation or elevation, they helped explain variation in surface fuels unexplained by lidar variables. Mapped total surface fuel loads increased with time since fire until about 10–15 years post fire, after which predicted fuel loads approached a steady state. Relatively fewer pixels had burned between 15 and 31 years previously in our study area (Fig. 4) so that the relationship between surface fuel load and time since fire that we reported is less reliable for that time period. Nevertheless, our asymptotic models are conceptually close to classic fire-driven fuel accumulation models such as Olson's negative exponential equation (Olson 1963; Birk and Simpson 1980; Keane 2015; Zazali et al. 2020). Likewise, previous field observation-based studies in ponderosa pine forests (Roccaforte et al. 2012) and mixed conifer forests (Dunn and Bailey 2015; Eskelson and Monleon, 2018; Stevens-Rumann et al. 2020) have documented similar asymptotic temporal trends in post-fire surface fuel loads that reached a steady state at 6–20 years post fire. Fine fuel accumulation is the balance between the input and the removal of fuels, mainly driven by litterfall and decomposition (Hanan et al. 2022). Litter accumulates on the soil until litterfall equals decomposition and accumulation stabilizes around a mean steady state (Ewel et al. 1976). Note as well that both decomposition and litterfall are

complex processes mainly driven by climate, aboveground biomass, site, and soil conditions (Prescott 2002; Bezkorovaynaya 2005; Krishna and Mohan 2017; Neumann et al. 2018; Costa et al. 2020). Changes to these can alter the system feedbacks and affect the accumulation process which would explain the fluctuation of fuel loads over the asymptote after a long time since fire (Fig. 4). In our study area, regions of lower productivity and therefore infrequent burning might also be responsible for seemingly stable fuel loads > 15 years post fire. To our knowledge, few studies have quantified the relationship between remote sensing-estimated fuel loads and time since fire. In longleaf pine forest in Florida, Hudak et al. (2016) also documented meaningful correlations between fuel loads estimated from airborne lidar and time since fire.

Differencing pre- and post-fire fuel load maps allowed us to estimate fuel consumption across fire extents. Both fires were dominated by low severity fire as indicated by MTBS dNBR (90–96%), which generally corresponds to non-crown fire in this area (Hoff et al. 2019); therefore, on average across fire extents, available canopy fuel was greater in 2020 than it was in 2019. Our maps did, however, document available canopy fuel consumption in areas that burned severely, as indicated by dNBR. Low canopy fuel consumption (average of  $0.07 \text{ Mg ha}^{-1}$  for pixels that burned severely) relative to surface fuel consumption (average of 14.0 and  $16.1 \text{ Mg ha}^{-1}$ ) was expected, as surface fuel loads were an order of magnitude greater. dNBR was moderately correlated with surface fuel consumption, but uncorrelated with canopy fuel consumption, likely because little to no canopy fuel burned in these fires which burned predominantly at low severity. For other

fires where crown fire is more prevalent, dNBR would likely be related more strongly to canopy fuel consumption. Our finding of moderate correlation between dNBR and surface fuel consumption suggests that dNBR could possibly be used as an index of surface fuel consumption for low-severity fires, although physically based estimates of consumption derived from pre- and post-fire lidar are likely superior. Our estimates of average fuel consumption ( $14.0\text{--}16.1\text{Mg ha}^{-1}$ ) and total surface fuel consumption ( $125.3 \pm 54.6$  and  $27.6 \pm 12.0$  Gg for the Castle and portion of the Ikes Fires, respectively) are similar in magnitude but less than those of McCarley et al. (2020), who estimated average total fuel consumptions of  $45\text{--}66\text{Mg ha}^{-1}$  and consumption totals ranging from 224 to 713 Gg for a portion of the 2011 Las Conchas Fire ( $49\text{ km}^2$ ) in New Mexico and the 2012 Pole Creek Fire ( $108\text{ km}^2$ ) in Oregon. As multitemporal lidar becomes more common, additional similar analyses estimating consumption will be possible. Such consumption estimates can increase our understanding of land/atmosphere exchanges of carbon.

## Conclusions

Airborne lidar, when combined with field observations, can be used to predict and map canopy and surface fuel loads with moderate accuracy across landscapes. We found that surface fuel loads were related to time since fire and present a remote sensing framework for quantifying landscape temporal dynamics in surface fuel accumulation. Our finding that fuel loads were related to time since fire suggests that future work that aims to map fuel loads with remote sensing can benefit from considering fire and other disturbance history.

Landscape scale fuel load maps derived from active remote sensing can provide unbiased geospatial decision support information to forest, wildland fire, and wildlife managers, helping them assess current conditions and plan future treatments for wildland fire risk reduction and long-term ecosystem resilience. As airborne lidar becomes more common in forested landscapes, our methods can also serve as a framework for estimating landscape scale fire emissions and assessing ecosystem dependent relationships, such as post disturbance fuel loading trajectories. The novel approaches described here can be especially useful in landscapes prone to uncharacteristically high severity wildfire due to climate change, such as the sky islands of the southwestern United States.

## Abbreviations

DBH: Diameter at breast height; dNBR: Differenced Normalized Burn Ratio; DTM: Digital terrain model; EVT: Existing Vegetation Type; Lidar: Light detection and ranging; MBE: Mean bias error; MIR: Normalized predictor variable importance score; MTBS: Monitoring Trends in Burn Severity; NPF: Number of past fires; RF: Random forest; RMSE: Root mean square error; %RMSE: Percent root mean square error; USFS: United States Forest Service; USNPS: United States National Park Service; YSF: Years since fire.

## Acknowledgements

Field observations are vital for remote sensing efforts such as this. For this project, we had planned to gather our own field observations for relation to airborne lidar data but were unable to because of COVID-19 travel restrictions. Without the existing field observations from USNPS and USFS monitoring programs, our analysis would not have been possible. We recommend that such field-based monitoring programs continue so that future remote sensing projects can be supported.

## Authors' contributions

BB and AH conceived and designed the analysis. BB, RM, and A. Spannuth gathered and processed data for the analysis. BB led the analysis. BB wrote the manuscript, with contributions from AH, RM, A. Spannuth, NS, and RO. A. Soja and RO provided funding and led the NASA FIRECHEM source fuel characterization and FASMEE study plan development work, respectively, that contributed to this study in support of FIREX-AQ (Grant number 80NSSC18K0685). All authors read and approved the final manuscript.

## Funding

This research was funded by the following: Fueled from below: Linking Fire, Fuels, and Weather to Atmospheric Chemistry (NASA Award 80NSSC18K0685); Furthering FIREX-AQ for Emissions Inventory and AQ Improvement (NASA Award 80HQTR21T0095); and the Joint Fire Science Program (JFSP) Fire and Smoke Model Evaluation Experiment (FASMEE) (Project 15-S-01-01).

## Availability of data and materials

The datasets used and analyzed during the current study are available from the corresponding author on reasonable request. Fuel load and consumption maps are available on WIFIRE Commons at <https://doi.org/10.48792/W2MW2V>.

## Declarations

### Ethics approval and consent to participate

Not applicable.

### Consent for publication

No applicable.

### Competing interests

The authors declare that they have no competing interests.

### Author details

<sup>1</sup>Rocky Mountain Research Station, USDA Forest Service, 1221 S Main Street, Moscow, ID 83843, USA. <sup>2</sup>College of Natural Resources, University of Idaho, 875 Perimeter Drive, Moscow, ID 83844, USA. <sup>3</sup>Kaibab National Forest, USDA Forest Service, 800 S 6th Street, Williams, AZ 86046, USA. <sup>4</sup>Pacific Northwest Research Station, USDA Forest Service, 400 N 34th Street, Suite 201, Seattle, WA 98103, USA. <sup>5</sup>National Institute of Aerospace, 100 Exploration Way, Hampton, VA 23666, USA. <sup>6</sup>NASA Langley Research Center, 21 Langley Blvd MS 420, Hampton, VA 23681, USA.

Received: 1 March 2022 Accepted: 15 July 2022

Published online: 09 August 2022

## References

- Alexander, Martin E., and Miguel G. Cruz. 2013. Limitations on the accuracy of model predictions of wildland fire behaviour: a state-of-the-knowledge overview. *The Forestry Chronicle* 89: 372–383. <https://doi.org/10.5558/ffc2013-067>.
- Alonso-Rego, Cecilia, Stéfano. Arellano-Pérez, Juan Guerra-Hernández, Juan A. Molina-Valero, Adela Martínez-Calvo, César. Pérez-Cruzado, Fernando Castedo-Dorado, Eduardo González-Ferreiro, Juan G. Álvarez-González, and Ana D. Ruiz-González. 2021. Estimating stand and fire-related surface and canopy fuel variables in pine stands using low-density airborne and single-scan terrestrial laser scanning data. *Remote Sensing* 13: 5170. <https://doi.org/10.3390/rs13245170>.
- Alonzo, Michael, Douglas C. Morton, Bruce D. Cook, Hans-Erik Andersen, Chad Babcock, and Robert Pattison. 2017. Patterns of canopy and surface layer

- consumption in a boreal forest fire from repeat airborne lidar. *Environmental Research Letters* 12: 065004. <https://doi.org/10.1088/1748-9326/aa6ade>.
- Andersen, Hans-Erik, Robert J. McGaughy, and Stephen E. Reutebuch. 2005. Estimating forest canopy fuel parameters using LIDAR data. *Remote Sensing of Environment* 94: 441–449. <https://doi.org/10.1016/j.rse.2004.10.013>.
- Arroyo, Lara A., Cristina Pascual, and José A. Manzanera. 2008. Fire models and methods to map fuel types: The role of remote sensing. *Forest Ecology and Management* 256: 1239–1252. <https://doi.org/10.1016/j.foreco.2008.06.048>.
- Bezkorovaynaya, I.N. 2005. The formation of soil invertebrate communities in the Siberian afforestation experiment. In *Tree species effects on soils: implications for global change*, 307–316. Dordrecht: Springer.
- Birk, Elaine M., and R.W. Simpson. 1980. Steady state and the continuous input model of litter accumulation and decomposition in Australian eucalypt forests. *Ecology* 61: 481–485. <https://doi.org/10.2307/1937411>.
- Breiman, Leo. 2001. Random forests. *Machine Learning* 45: 5–32. <https://doi.org/10.1023/A:1010933404324>.
- Bright, Benjamin C., Andrew T. Hudak, Arjan J.H. Meddens, Todd J. Hawbaker, Jennifer S. Briggs, and Robert E. Kennedy. 2017. Prediction of forest canopy and surface fuels from lidar and satellite time series data in a bark beetle-affected forest. *Forests* 8: 322. <https://doi.org/10.3390/f8090322>.
- Brown, James K. 1974. *Handbook for inventorying downed woody material*. General Technical Report GTR-INT-16, 24. Ogden: USDA Forest Service, Intermountain Forest and Range Experiment Station.
- Brown, James K., Rick D. Oberheu, and Cameron M. Johnston. 1982. *Handbook for inventorying surface fuels and biomass in the Interior West*. General Technical Report INT-129, 48. Ogden: USDA Forest Service, Intermountain Forest and Range Experiment Station.
- Costa, Alan N., Jeane R. Souza, Karyne M. Alves, Anderson Penna-Oliveira, Geisciele Paula-Silva, Ingrid S. Becker, Kelly Marinho-Vieira, Ana L. Bonfim, Alessandra Bartimachi, and Ernane H.M. Vieira-Neto. 2020. Linking the spatiotemporal variation of litterfall to standing vegetation biomass in Brazilian savannas. *Journal of Plant Ecology* 13: 517–524. <https://doi.org/10.1093/jpe/rtaa039>.
- Countryman, Clive M. 1972. *The fire environment concept*, 12. Berkeley: USDA Forest Service, Pacific Southwest Forest and Range Experiment Station.
- Covington, W. Wallace, Richard L. Everett, Robert Steele, Larry L. Irwin, Tom A. Daer, and Allan N.D. Auclair. 1994. Historical and anticipated changes in forest ecosystems of the inland west of the United States. *Journal of Sustainable Forestry* 2: 13–63. [https://doi.org/10.1300/J091v02n01\\_02](https://doi.org/10.1300/J091v02n01_02).
- Dunn, Christopher J., and John D. Bailey. 2015. Temporal fuel dynamics following high-severity fire in dry mixed conifer forests of the eastern Cascades, Oregon, USA. *International Journal of Wildland Fire* 24 (4): 470–483. <https://doi.org/10.1071/WF13139>.
- Eidenshink, Jeff, Brian Schwind, Ken Brewer, Zhi-Liang. Zhu, Brad Quayle, and Stephen Howard. 2007. A project for monitoring trends in burn severity. *Fire Ecology* 3: 3–21. <https://doi.org/10.4996/fireecology.0301003>.
- Erdody, Todd L., and L. Monika Moskal. 2010. Fusion of LiDAR and imagery for estimating forest canopy fuels. *Remote Sensing of Environment* 114: 725–737. <https://doi.org/10.1016/j.rse.2009.11.002>.
- Eskelson, Bianca N.I., and Vicente J. Monleon. 2018. Post-fire surface fuel dynamics in California forests across three burn severity classes. *International Journal of Wildland Fire* 27: 114–124. <https://doi.org/10.1071/WF17148>.
- Evans, Jeffrey S. 2021. *spatialEco*. R package version 1.3-6 <https://github.com/jeffrejevans/spatialEco>.
- Evans, Jeffrey S., and A. Melanie Murphy. 2018. *rfUtilities*. R package version 2.1-3 <https://cran.r-project.org/package=rfUtilities>.
- Ewel, John J. 1976. Litter fall and leaf decomposition in a tropical forest succession in eastern Guatemala. *The Journal of Ecology* 64: 293–308. <https://doi.org/10.2307/2258696>.
- French, Nancy H.F., Pierre Goovaerts, and Eric S. Kasischke. 2004. Uncertainty in estimating carbon emissions from boreal forest fires. *Journal of Geophysical Research: Atmospheres* 109 (14): 14–8. <https://doi.org/10.1029/2003JD003635>.
- Fulé, Peter Z., Thomas A. Heinlein, W. Wallace. Covington, and Margaret M. Moore. 2003a. Assessing fire regimes on Grand Canyon landscapes with fire-scar and fire-record data. *International Journal of Wildland Fire* 12: 129–145. <https://doi.org/10.1071/WF02060>.
- Fulé, Peter Z., Joseph E. Crouse, Thomas A. Heinlein, Margaret M. Moore, W. Wallace Covington, and Greg Verkamp. 2003b. Mixed-severity fire regime in a high-elevation forest of Grand Canyon, Arizona, USA. *Landscape Ecology* 18 (5): 465–486. <https://doi.org/10.1023/A:1026012118011>.
- García, Mariano, Sorin Popescu, David Riaño, Kaiguang Zhao, Amy Neuen-schwander, Muge Agca, Emilio Chuvieco. 2012. Characterization of canopy fuels using ICESat/GLAS data. *Remote Sensing of Environment* 123: 81–89. <https://doi.org/10.1016/j.rse.2012.03.018>.
- Graham, Russell T., Sarah McCaffrey, and Theresa B. Jain. 2004. *Science basis for changing forest structure to modify wildfire behavior and severity*. General Technical Report RMRS-GTR-120, 43. USDA Forest Service, Rocky Mountain Research Station: Fort Collins.
- Hanan, Erin J., Maureen C. Kennedy, Jianning Ren, Morris C. Johnson, and Alistair M.S. Smith. 2022. Missing climate feedbacks in fire models: limitations and uncertainties in fuel loadings and the role of decomposition in fine fuel accumulation. *Journal of Advances in Modeling Earth Systems* 14: e2021MS002818. <https://doi.org/10.1029/2021MS002818>.
- Hawley, Christie M., E. Louise Loudermilk, Eric M. Rowell, and Scott Pokswinski. 2018. A novel approach to fuel biomass sampling for 3D fuel characterization. *MethodsX* 5: 1597–1604. <https://doi.org/10.1016/j.mex.2018.11.006>.
- Hermosilla, Txomin, Luis A. Ruiz, Alexandra N. Kazakova, Nicholas C. Coops, and L. Monika Moskal. 2013. Estimation of forest structure and canopy fuel parameters from small-footprint full-waveform LiDAR data. *International Journal of Wildland Fire* 23: 224–233. <https://doi.org/10.1071/WF13086>.
- Hiers, J. Kevin, Joseph J. O'Brien, R.J. Mitchell, John M. Grego, and E. Louise Loudermilk. 2009. The wildland fuel cell concept: an approach to characterize fine-scale variation in fuels and fire in frequently burned longleaf pine forests. *International Journal of Wildland Fire* 18: 315–325. <https://doi.org/10.1071/WF08084>.
- Hiers, J. Kevin, Joseph J. O'Brien, J. Morgan Varner, Bret W. Butler, Matthew Dickinson, James Furman, Michael Gallagher, David Godwin, Scott L. Goodrick, Sharon M. Hood, Andrew Hudak, Leda N. Kobziar, Rodman Linn, E. Louise Loudermilk, Sarah McCaffrey, Kevin Robertson, Eric M. Rowell, Nicholas Skowronski, Adam C. Wattsand, and Kara M. Yedinak. 2020. Prescribed fire science: the case for a refined research agenda. *Fire Ecology* 16: 11. <https://doi.org/10.1186/s42408-020-0070-8>.
- Hijmans, Robert J. 2021a. *raster: geographic data analysis and modeling*. R package version 3.4-13 <https://CRAN.R-project.org/package=raster>.
- Hijmans, Robert J. 2021b. *terra: spatial data analysis*. R package version 1.3-4 <https://CRAN.R-project.org/package=terra>.
- Hoe, Michael S., Christopher J. Dunn, and Halemariam Temesgen. 2018. Multitemporal LiDAR improves estimates of fire severity in forested landscapes. *International Journal of Wildland Fire* 27: 581–594. <https://doi.org/10.1071/WF17141>.
- Hoff, Valentijn, Eric Rowell, Casey Teske, Lloyd Queen, and Tim Wallace. 2019. Assessing the relationship between forest structure and fire severity on the North Rim of the Grand Canyon. *Fire* 2: 10. <https://doi.org/10.3390/fire2010010>.
- Hu, Tianyu, Qin Ma, Yanjun Su, John J. Battles, Brandon M. Collins, Scott L. Stephens, Maggi Kelly, and Qinghua Guo. 2019. A simple and integrated approach for fire severity assessment using bi-temporal airborne LiDAR data. *International Journal of Applied Earth Observation and Geoinformation* 78: 25–38. <https://doi.org/10.1016/j.jag.2019.01.007>.
- Hudak, Andrew T., Matthew B. Dickinson, Benjamin C. Bright, Robert L. Kremens, E. Louise Loudermilk, Joseph J. O'Brien, and Roger D. Ottmar. 2015. Measurements relating fire radiative energy density and surface fuel consumption – RxCADRE 2011 and 2012. *International Journal of Wildland Fire* 25: 25–37. <https://doi.org/10.1071/WF14159>.
- Hudak, Andrew T., Benjamin C. Bright, Scott M. Pokswinski, E. Louise Loudermilk, Joseph J. O'Brien, Benjamin S. Hornsby, Carine Klauberg, and Carlos A. Silva. 2016. Mapping forest structure and composition from low density lidar for informed forest, fuel, and fire management at Eglin Air Force Base, Florida, USA. *Canadian Journal of Remote Sensing* 42: 411–427. <https://doi.org/10.1080/07038992.2016.1217482>.
- Hudak, Andrew T., Akira Kato, Benjamin C. Bright, E. Louise Loudermilk, Christie Hawley, Joseph C. Restaino, Roger D. Ottmar, Gabriel A. Prata, Carlos Cabo, Susan J. Prichard, Eric M. Rowell, and David R. Weise. 2020. Towards spatially explicit quantification of pre- and postfire fuels and fuel consumption from traditional and point cloud measurements. *Forest Science* 66: 428–442. <https://doi.org/10.1093/forsci/fxz085>.

- Isenburg, Martin. 2021. *LAStools - efficient LiDAR processing software (version 202216, academic)*<http://rapidlasso.com/LAStools>.
- Jakubowski, Marek K., Qinghua Guo, Brandon Collins, Scott Stephens, and Maggi Kelly. 2013. Predicting surface fuel models and fuel metrics using Lidar and CIR imagery in a dense, mountainous forest. *Photogrammetric Engineering & Remote Sensing* 79: 37–49. <https://doi.org/10.14358/PERS.79.1.37>.
- Keane, Robert E. 2015. *Wildland fuel fundamentals and applications*, 202. New York: Springer.
- Keane, Robert E., Scott A. Mincemoyer, Kirsten M. Schmidt, Donald G. Long, and Janice L. Garner. 2000. *Mapping vegetation and fuels for fire management on the Gila National Forest Complex, New Mexico. General Technical Report RMRS-GTR-46*, 126. Ogden: USDA Forest Service, Rocky Mountain Research Station.
- Keane, Robert E., Robert Burgan, and Jan van Wagtenonk. 2001. Mapping wildland fuels for fire management across multiple scales: integrating remote sensing, GIS, and biophysical modeling. *International Journal of Wildland Fire* 10: 301–319. <https://doi.org/10.1071/WF01028>.
- Key, Carl H., and Nathan C. Benson. 2006. Landscape assessment (LA). In *FIREMON: fire effects monitoring and inventory system. Gen. Tech. Rep. RMRS-GTR-164-CD*, ed. Duncan C. Lutes, Robert E. Keane, John F. Caratti, Carl H. Key, Benson Nathan C, Steve Sutherland, and Larry J. Gangi, LA-1-55 164. Fort Collins: USDA Forest Service, Rocky Mountain Research Station.
- Krishna, M.P., and Mahesh Mohan. 2017. Litter decomposition in forest ecosystems: a review. *Energy Ecology and Environment* 2: 236–249. <https://doi.org/10.1007/s40974-017-0064-9>.
- LANDFIRE. 2014. *Existing vegetation type layer, LANDFIRE 1.4.0*. U.S. Department of the Interior, Geological Survey, and U.S. Department of Agriculture. <http://landfire.cr.usgs.gov/viewer/>. Accessed Sept 2021.
- LANDFIRE. 2016. *Existing vegetation type layer, LANDFIRE 2.0.0*. U.S. Department of the Interior, Geological Survey, and U.S. Department of Agriculture. <http://landfire.cr.usgs.gov/viewer/>. Accessed Sept 2021.
- Leenhouts, Bill. 1998. Assessment of biomass burning in the conterminous United States. *Conservation Ecology* 2. <https://www.ecologyandsociety.org/vol2/iss1/art1/inline.html>.
- Leite, Rodrigo Vieira, Carlos Alberto Silva, Eben North Broadbent, Cibele Hummel do Amaral, Veraldo Liesenberg, Danilo Roberti Alves, de Almeida, Midhun Mohan, Sérgio. Godinho, Adrian Cardil, Caio Hamamura, Bruno Lopes de Faria, Pedro H.S. Brancalion, André Hirsch, Gustavo Eduardo Marcatti, Ana Paula Dalla. Corte, Angelica Maria Almeyda. Zambrano, Máira Beatriz Teixeira. da Costa, Eraldo Aparecido Trondoli. Matricardi, Anne Laura da Silva, Lucas Ruggeri Ré Y. Goya, Ruben Valbuena, Bruno Araujo Furtado, de Mendonça, Celso H.L. Silva Junior, Luiz E.O.C. Aragão, Mariano García, Jingjing Liang, Trina Merrick, Andrew T. Hudak, Jingfeng Xiao, Steven Hancock, Laura Duncason, Matheus Pinheiro Ferreira, Denis Valle, Sassan Saatchi, and Carine Klauberg. 2022. Large scale multi-layer fuel load characterization in tropical savanna using GEDI spaceborne lidar data. *Remote Sensing of Environment* 268: 112764. <https://doi.org/10.1016/j.rse.2021.112764>
- Liaw, Andy, and Matthew Wiener. 2002. Classification and regression by random forest. *R News* 2: 18–22.
- Lin, Chinsu, Siao-En. Ma, Li-Ping. Huang, Chung-I. Chen, Pei-Ting. Lin, Zhih-Kai. Yang, and Kuan-Ting. Lin. 2021. Generating a baseline map of surface fuel loading using stratified random sampling inventory data through cokriging and multiple linear regression methods. *Remote Sensing* 13: 1561. <https://doi.org/10.3390/rs13081561>.
- López-Senespleda, Eduardo, Rafael Calama, and Ricardo Ruiz-Peinado. 2021. Estimating forest floor carbon stocks in woodland formations in Spain. *Science of The Total Environment* 788: 147734. <https://doi.org/10.1016/j.scitotenv.2021.147734>.
- Loudermilk, E. Louise, J. Kevin Hiers, Joseph J. O'Brien, Robert J. Mitchell, Abhinav Singhania, Juan C. Fernandez, Wendell P. Cropper Jr., and K. Clint. Slatton. 2009. Ground-based LIDAR: a novel approach to quantify fine-scale fuelbed characteristics. *International Journal of Wildland Fire* 18: 676–685. <https://doi.org/10.1071/WF07138>.
- Lutes, Duncan. 2021. *FuelCalc User's Guide (version 1.7)*<https://www.firelab.org/project/fuelcalc>.
- Lydersen, Jamie M., Brandon M. Collins, Eric E. Knapp, Gary B. Roller, and Scott Stephens. 2015. Relating fuel loads to overstorey structure and composition in a fire-excluded Sierra Nevada mixed conifer forest. *International Journal of Wildland Fire* 24: 484–494. <https://doi.org/10.1071/WF13066>.
- Mauro, Francisco, Andrew T. Hudak, Patrick A. Fekety, Bryce Frank, Hailemariam Temesgen, David M. Bell, Matthew J. Gregory, and T.R. McCarley. 2021. Regional modeling of forest fuels and structural attributes using airborne laser scanning data in Oregon. *Remote Sensing* 13: 261. <https://doi.org/10.3390/rs13020261>.
- McCarley, T Ryan, Andrew T. Hudak, Aaron M. Sparks, Nicole M. Vaillant, Arjan J.H. Meddens, Laura Trader, Francisco Mauro, Jason Kreitler, and Luigi Boschetti. 2020. Estimating wildfire fuel consumption with multitemporal airborne laser scanning data and demonstrating linkage with MODIS-derived fire radiative energy. *Remote Sensing of Environment* 251: 112114. <https://doi.org/10.1016/j.rse.2020.112114>.
- McCune, Bruce, and Dylan Keon. 2002. Equations for potential annual direct incident radiation and heat load index. *Journal of Vegetation Science* 13: 603–606. <https://doi.org/10.1111/j.1654-1103.2002.tb02087.x>.
- Murphy, Melanie A., Jeffrey S. Evans, and Andrew Storfer. 2010. Quantifying Bufo boreas connectivity in Yellowstone National Park with landscape genetics. *Ecology* 91: 252–261. <https://doi.org/10.1890/08-0879.1>.
- Neumann, Mathias, Liisa Ukonmaanaho, James Johnson, Sue Benham, Lars Vesterdal, Radek Novotný, Arne Verstraeten, Lars Lundin, Anne Thimonier, Panagiotis Michopoulos, and Hubert Hasenauer. 2018. Quantifying carbon and nutrient input from litterfall in European forests using field observations and modeling. *Global Biogeochemical Cycles* 32: 784–798. <https://doi.org/10.1029/2017GB005825>.
- Olson, Jerry S. 1963. Energy storage and the balance of producers and decomposers in ecological systems. *Ecology* 44: 322–331. <https://doi.org/10.2307/1932179>.
- Ottmar, Roger D., David V. Sandberg, Cynthia L. Riccardi, and Susan J. Prichard. 2007. An overview of the fuel characteristic classification system—quantifying, classifying, and creating fuelbeds for resource planning. *Canadian Journal of Forest Research* 37: 2383–2393. <https://doi.org/10.1139/X07-077>.
- Pesonen, Annukka, Matti Maltamo, Kalle Eerikäinen, and Petteri Packalén. 2008. Airborne laser scanning-based prediction of coarse woody debris volumes in a conservation area. *Forest Ecology and Management* 255: 3288–3296. <https://doi.org/10.1016/j.foreco.2008.02.017>.
- Peterson, Birgit, Kurtis Nelson, and Bruce Wylie. 2013. Towards integration of GLAS into a national fuel mapping program. *Photogrammetric Engineering & Remote Sensing* 79: 175–183. <https://doi.org/10.14358/PERS.79.2.175>.
- Pierce, Andrew D., Calvin A. Farris, and Alan H. Taylor. 2012. Use of random forests for modeling and mapping forest canopy fuels for fire behavior analysis in Lassen Volcanic National Park, California, USA. *Forest Ecology and Management* 279: 77–89. <https://doi.org/10.1016/j.foreco.2012.05.010>.
- Prescott, Cindy E. 2002. The influence of the forest canopy on nutrient cycling. *Tree Physiology* 22: 1193–1200. <https://doi.org/10.1093/treephys/22.15-16.1193>.
- Price, Owen F., and Christopher E. Gordon. 2016. The potential for LiDAR technology to map fire fuel hazard over large areas of Australian forest. *Journal of Environmental Management* 181: 663–673. <https://doi.org/10.1016/j.jenvman.2016.08.042>.
- R Core Team. 2021. *R: a language and environment for statistical computing*. Vienna: R Foundation for Statistical Computing <https://www.R-project.org/>.
- Reeves, Matthew C., Kevin C. Ryan, Matthew G. Rollins, and Thomas G. Thompson. 2009. Spatial fuel data products of the LANDFIRE project. *International Journal of Wildland Fire* 18: 250–267. <https://doi.org/10.1071/WF08086>.
- Reich, Robin M., John E. Lundquist, and Vanessa A. Bravo. 2004. Spatial models for estimating fuel loads in the Black Hills, South Dakota, USA. *International Journal of Wildland Fire* 13: 119–129. <https://doi.org/10.1071/WF02049>.
- Reinhardt, Elizabeth, Duncan Lutes, and Joe Scott. 2006. FuelCalc: a method for estimating fuel characteristics. In: Andrews, Patricia L. and Bret W. Butler, comps. 2006. *Fuels management-how to measure success: conference proceedings. 28-30 March 2006; Portland, OR. Proceedings RMRS-P-41*. Fort Collins: USDA Forest Service, Rocky Mountain Research Station. p. 273–282.
- Roberts, D.W., and S.V. Cooper. 1989. *Concepts and techniques of vegetation mapping. Land classifications based on vegetation - applications for resource management. General Technical Report INT-257*, 90–96. Ogden: USDA Forest Service.
- Rocafort, John P., Peter Z. Fulé, W. Walker Chancellor, and Daniel C. Laughlin. 2012. Woody debris and tree regeneration dynamics following severe wildfires in Arizona ponderosa pine forests. *Canadian Journal of Forest Research* 42: 593–604. <https://doi.org/10.1139/x2012-010>.
- Rollins, Matthew G. 2009. LANDFIRE: a nationally consistent vegetation, wildland fire, and fuel assessment. *International Journal of Wildland Fire* 18: 235–249. <https://doi.org/10.1071/WF08088>.

- Rowell, Eric, E. Louise Loudermilk, Carl Seielstad, and Joseph J. O'Brien. 2016. Using simulated 3D surface fuelbeds and terrestrial laser scan data to develop inputs to fire behavior models. *Canadian Journal of Remote Sensing* 42: 443–459. <https://doi.org/10.1080/07038992.2016.1220827>.
- Rowell, Eric, E. Louise Loudermilk, Christie Hawley, Scott Pokswinski, Carl Seielstad, Lloyd Queen, Joseph J. O'Brien, Andrew T. Hudak, Scott Goodrick, and J. Kevin Hiers. 2020. Coupling terrestrial laser scanning with 3D fuel biomass sampling for advancing wildland fuels characterization. *Forest Ecology and Management* 462: 117945. <https://doi.org/10.1016/j.foreco.2020.117945>.
- Seielstad, Carl A., and Lloyd P. Queen. 2003. Using airborne laser altimetry to determine fuel models for estimating fire behavior. *Journal of Forestry* 101: 10–15. <https://doi.org/10.1093/jof/101.4.10>.
- Seiler, Wolfgang, and Paul J. Crutzen. 1980. Estimates of gross and net fluxes of carbon between the biosphere and the atmosphere from biomass burning. *Climatic Change* 2: 207–247. <https://doi.org/10.1007/BF00137988>.
- Skowronski, N.S., K.L. Clark, M. Duveneck, and J. Hom. 2011. Three-dimensional canopy fuel loading predicted using upward and downward sensing LiDAR systems. *Remote Sensing of Environment* 115: 703–714. <https://doi.org/10.1016/j.rse.2010.10.012>.
- Skowronski, Nicholas S., Michael R. Gallagher, and Timothy A. Warner. 2020. Decomposing the interactions between fire severity and canopy fuel structure using multi-temporal, active, and passive remote sensing approaches. *Fire* 3: 7. <https://doi.org/10.3390/fire3010007>.
- Stage, A.I.R. 1976. An expression of the effects of aspect, slope, and habitat type on tree growth. *Forest Science* 22: 457–460.
- Stefanidou, Alexandra, Ioannis Z. Gitas, Lauri Korhonen, Nikos Georgopoulos, and Dimitris Stavrakoudis. 2020. Multispectral LiDAR-based estimation of surface fuel load in a dense coniferous forest. *Remote Sensing* 12: 3333. <https://doi.org/10.3390/rs12203333>.
- Stevens-Rumann, Camille S., Andrew T. Hudak, Penelope Morgan, Alex Arnold, and Eva K. Strand. 2020. Fuel dynamics following wildfire in US Northern Rockies forests. *Frontiers in Forests and Global Change* 3: 51. <https://doi.org/10.3389/ffgc.2020.00051>.
- Strobl, Carolin, Anne-Laure Boulesteix, Thomas Kneib, Thomas Augustin, and Achim Zeileis. 2008. Conditional variable importance for random forests. *BMC Bioinformatics* 9: 1–11. <https://doi.org/10.1186/1471-2105-9-307>.
- USDA Forest Service. 2014. *Land and resource management plan for the Kaibab National Forest, Coconino, Yavapai, and Mojave Counties, Arizona*. [https://www.fs.usda.gov/Internet/FSE\\_DOCUMENTS/fseprd517406.pdf](https://www.fs.usda.gov/Internet/FSE_DOCUMENTS/fseprd517406.pdf).
- USDA Forest Service. 2020. *Kaibab plateau ecological restoration projects, environmental assessment*. [https://www.fs.usda.gov/nfs/11558/www/nepa/109549\\_FSPLT3\\_5314654.pdf](https://www.fs.usda.gov/nfs/11558/www/nepa/109549_FSPLT3_5314654.pdf).
- USDOI National Park Service. 2010. *F. Appendix: Grand Canyon National Park wildland and prescribed fire monitoring and research plan. Prep. By Windy Bunn*.
- Wang, Cheng, and Nancy F. Glenn. 2009. Estimation of fire severity using pre- and post-fire LiDAR data in sagebrush steppe rangelands. *International Journal of Wildland Fire* 18: 848–856. <https://doi.org/10.1071/WF08173>.
- Wilson, Margaret F.J., Brian O'Connell, Colin Brown, Janine C. Guinan, and Anthony J. Grehan. 2007. Multiscale terrain analysis of multibeam bathymetry data for habitat mapping on the continental slope. *Marine Geodesy* 30: 3–35. <https://doi.org/10.1080/01490410701295962>.
- Zazali, Hilyati H., Isaac N. Towers, and Jason J. Sharples. 2020. A critical review of fuel accumulation models used in Australian fire management. *International Journal of Wildland Fire* 30: 42–56. <https://doi.org/10.1071/WF20031>.
- Zevenbergen, Lyle W., and Colin R. Thorne. 1987. Quantitative analysis of land surface topography. *Earth Surface Processes and Landforms* 12: 47–56. <https://doi.org/10.1002/esp.3290120107>.

## Publisher's Note

Springer Nature remains neutral with regard to jurisdictional claims in published maps and institutional affiliations.

Submit your manuscript to a SpringerOpen<sup>®</sup> journal and benefit from:

- Convenient online submission
- Rigorous peer review
- Open access: articles freely available online
- High visibility within the field
- Retaining the copyright to your article

---

Submit your next manuscript at ► [springeropen.com](https://www.springeropen.com)

---